



# Characteristic traffic load effects from a mixture of loading events on short to medium span bridges

Colin C. Caprani <sup>a,\*</sup>, Eugene J. OBrien <sup>b</sup>, Geoff J. McLachlan <sup>c</sup>

<sup>a</sup> *Department of Civil/Structural Engineering, Dublin Institute of Technology, Bolton Street, Dublin 2, Ireland*

<sup>b</sup> *School Urban Institute Ireland, University College Dublin, Dublin 4, Ireland*

<sup>c</sup> *Department of Statistics, University of Queensland, Brisbane 4072, Australia*

Received 29 June 2005; received in revised form 22 March 2006; accepted 21 November 2006

## Abstract

In recent years, highway bridge load assessment has been recognised as an area through which savings can be made by avoiding unnecessary bridge refurbishment and replacement. Load effects in bridges result from single truck crossings or multiple-truck presence events which are, statistically, not identically distributed. Conventional approaches fit statistical distributions to mixtures of non-identically distributed load effects. Inaccuracies in the conventional approach are identified and an alternative approach is developed to find the characteristic load effects. Theoretical and field data are used to show the potential implications of conventional techniques and to demonstrate the application of the new approach.

© 2007 Published by Elsevier Ltd.

*Keywords:* Bridge; Assessment; Statistics; Extreme value; Traffic; Load

## 1. Introduction

In recent years, increasingly sophisticated approaches to the assessment of bridges have emerged in an effort to minimise unnecessary repair or replacement of existing structures. Considerable attention has been given to the assessment of the load carrying capacity of bridges and it is possible to assess carrying capacity reasonably accurately. However, particularly for less heavily trafficked bridges, there is often greater potential for savings in an accurate assessment of the actual traffic loading at the bridge site. In some countries, a notional assessment traffic load model is specified which can include allowance for load differences between sites (see, for example [1,2]). However, such models are necessarily conservative as they are still applicable to a number of bridges and are therefore deemed to represent a wide range of traffic conditions. Bridges can often be shown to be safe for the individual site-specific traffic loading to which they are subject, even if they do not have the capacity to resist the notional assessment load for the network or road class. It is this site-specific assessment of traffic load that is the subject of this paper.

\* Corresponding author.

*E-mail addresses:* [colin.caprani@dit.ie](mailto:colin.caprani@dit.ie) (C.C. Caprani), [eugene.obrien@ucd.ie](mailto:eugene.obrien@ucd.ie) (E.J. OBrien), [gjm@maths.uq.edu.au](mailto:gjm@maths.uq.edu.au) (G.J. McLachlan).

When the statistics of the traffic is available, Monte Carlo methods may be used to generate periods of synthetic traffic which are considerably longer than the original measurement period, but which will have the same statistical characteristics. These traffic streams are used to generate the bridge loading history for the time period of the stream. However, the limitations of the Monte Carlo method must be borne in mind when performing such simulations [3].

A load effect on a bridge is any effect, such as bending moment or strain, which results from any form of loading event. This study is limited to load effects in short- to medium-span (20–50 m), bidirectional, two-lane bridges. For these bridge lengths, when an allowance for dynamic effects is made, free-flowing traffic is assumed to generally govern [4]. The conventional approach used by many authors is to identify the maximum load effect recorded during a loading event [5,6] or in a reference period such as a day [2,8–10] or a week [11], and to fit these maxima to an extreme value distribution. This approach is based on the assumption that individual loading events are independent and identically distributed (iid) [13,14]. However, load effects can be the result of any of a number of quite different loading events, involving different numbers of trucks. A single truck crossing event is relatively simple with variables of truck weight, axle configuration and distribution of weight between axles. Events involving two trucks are more complex involving distributions for weight and geometric variables for both trucks and new statistical variables such as the location of the second truck relative to the first. It is therefore clear that, in general, a load effect due to the passage of a single vehicle has a different distribution to the same load effect due to an occurrence of multiple vehicles. To mix load effects from such different loading events violates the iid assumption used in extreme value analysis. This paper addresses such mixing of non-iid load effects. Theoretical examples using known distributions for the different sources of load effect are used to show the errors that can result from fittings to mixtures. Results from the two approaches are compared using data from a Weigh-in-Motion site.

## 2. Statistics of traffic loading

### 2.1. Probability by event type

A bridge loading event (BLE) is defined as the presence for a continuous period of time of at least one truck on the influence area of the load effect of interest. BLEs are classified here on the basis of the number of trucks that contribute to the maximum load effect recorded during the event. Single truck loading events are considerably more frequent than events involving more trucks but the mean value of load effect is relatively small as the gross vehicle weight (GVW) of individual trucks is limited. Multiple-truck loading events are rarer, but the combined weight of the multiple trucks can be much higher, so the load effect tends to be larger. Other truck characteristics also affect the resulting load effect, such as axle spacing, but GVW serves as the primary indicator.

The BLE sample space can be partitioned into  $j$ -truck loading events, where  $n_j$  is the maximum possible number of trucks contributing to a maximum load effect. The probability that the maximum load effect in the  $i$ th event of BLEs in a given reference period such as a day,  $S_i$ , is less than or equal to some value,  $s$ , is then given by the Law of Total Probability:

$$P[S_i \leq s] = \sum_{j=1}^{n_i} F_j(s) \cdot f_j \quad (1)$$

where  $F_j(\cdot)$  is the cumulative distribution function for the maximum load effect in a  $j$ -truck event and  $f_j$  is the probability of occurrence of a  $j$ -truck event. The maximum value for all events in the reference period is denoted by  $\hat{S}$ ; for example, the maximum-per-day load effect. The probability that  $\hat{S}$  is less than or equal to some value  $s$  is given by:

$$P[\hat{S} \leq s] = P[\max_{i=1}^{n_d} (S_i \leq s)] = \prod_{i=1}^{n_d} P[S_i \leq s] \quad (2)$$

This assumes that individual BLEs are independent. Substitution of (1) into (2) gives

$$P[\widehat{S} \leq s] = \left( \sum_{j=1}^{n_d} F_j(s) \cdot f_j \right)^{n_d} \quad (3)$$

The number of BLEs per day,  $n_d$ , is a random variable, and is in general different each day. However, there is little loss of accuracy in assuming its expected value, provided it is sufficiently large (see, for example [15]).

An approach has been presented by several authors which combines the effects of multiple statistical generating mechanisms operating on the same random variables, and is presented as Eq. (4), in which  $G_j(s)$  is an extreme value distribution of the  $j$ th loading event type:

$$P[\widehat{S} \leq s] = \prod_{j=1}^{n_d} G_j(s) \quad (4)$$

Gomes and Vickery [15] present this equation without derivation; Gumbel [12] deals with the particular case of two mechanisms; Harman and Davenport [16] begin with a consideration of mutually exclusive loading events and arrive at a similar result; and Cook et al. [17] arrive at it from considerations close to those here. Eq. (3) is presented in this paper and Appendix I demonstrates the necessary and sufficient conditions for convergence of Eq. (3) to Eq. (4).

Assuming convergence to generalised extreme value (GEV) distributions,  $G_j(s)$  is of GEV form [18]:

$$G_j(s) = \exp \left\{ - \left[ 1 - \xi_j \left( \frac{s - \mu_j}{\sigma_j} \right) \right]^{1/\xi_j} \right\} \quad (5)$$

where  $\mu_j$  is the location parameter;  $\sigma_j$  the scale parameter; and  $\xi_j$  the shape parameter – all for loading event type  $j$ . Hence, Eq. (4) becomes

$$P[\widehat{S} \leq s] = \exp[-h(s)] \quad (6)$$

where

$$h(s) = \sum_{j=1}^{n_d} \left[ 1 - \xi_j \left( \frac{s - \mu_j}{\sigma_j} \right) \right]^{1/\xi_j} \quad (7)$$

The parameters of the distributions are determined by fits to each BLE type separately.

A theoretical comparison of Eq. (4) with the conventional approach [12,5–10] described previously is difficult. Most of the statistical literature deals with likelihood ratio tests for nested models [19]. There are tests for non-nested models such as that of Voung [20]. Unfortunately these tests do not strictly apply in this particular case as the distributions for comparison are derived from different data and a different number of data points. Comparison of the fits to the daily maxima is misleading – the conventional approach will generally be better as the new approach is not fitted to the overall daily maxima, rather the daily maxima of the particular loading event type.

## 2.2. Theoretical examples

Three examples are considered where the parent distributions,  $F_j$ , for each event type,  $j$ , are stipulated. Hence, the exact solutions can be calculated from Eq. (3) and used to assess the accuracy of the two approaches. It is shown in Section 3 that load effect data for the  $i$ th event type,  $S_i$ , fit well to the GEV distribution. Hence, for these examples, the parent distributions are chosen as GEV distributions. It is important to note that these event types do not represent real loading event-types, but are merely used to illustrate the consequences of the application of the conventional and current approach to different data sets.

In Example 1, three loading event types exist with the parameters given in Table 1. The probabilities of occurrence,  $f_j$ , of each event type, also given in the table, reduce from types 1 to 3. Type 1 events are more than twice as probable as type 2 events and type 3 events only occur 2% of the time. The total number of events per day (of all types) is specified as  $n_d = 2800$ .

Table 1  
Properties of parent distributions

Example	$n_d$	Event type number	Distribution properties (GEV)			Probability of occurrence, $f_j$
			Location $\mu$	Scale $\sigma$	Shape $\xi$	
1	2800	Type 1	370	31	-0.07	0.7
		Type 2	300	127	0.19	0.28
		Type 3	380	128	0.19	0.02
2	800	Type 1	610	270	0.18	0.95
		Type 2	840	310	0.21	0.05
3	2000	Type 1	3500	265	-0.1	0.98
		Type 2	3600	1400	0.2	0.02

Assuming 250 working days per year and a 1000-year return period (consistent with Eurocode 1.3 [21]), the characteristic load effect of maximum-per-day load effect is that value with probability of exceedance 1 in  $250 \times 10^3$ . Substituting the parameters of Table 1 into Eq. (3) and equating to a probability of  $1 - 1/250 \times 10^3$  gives the characteristic value for  $s$  of  $s_k = 1724$  (where the subscript  $k$  denotes the characteristic value of load effect). This value is exact as it is calculated from the known statistical distributions defined in Table 1.

The accuracy of using Eq. (4) and the conventional approach is assessed using the known solution. To apply Eq. (4), Monte-Carlo simulation is used to sample the distributions for each of the event-types of Table 1. This is repeated for a total of 1000 days to obtain a 1000-day sample, representative of the quantity of data that might typically be available. GEV distributions fit well to the maximum-per-day data for each of the event types. The type 2 and type 3 event distributions in this example have positive shape factors,  $\xi$ . The distributions therefore curve upwards and will be bounded by upper limits, regardless of the number of repetitions. The type 1 event data have a negative shape factor and this distribution crosses the others well within the data simulated. Hence, the type 1 event daily maxima coincide with overall daily maxima for many of the greater 'load effects'.

Fig. 1a shows the data and the three GEV fits. The probabilities of exceedance by any of these three event-types are combined using Eqs. (6) and (7). This combined distribution is also plotted in Fig. 1a. When the level

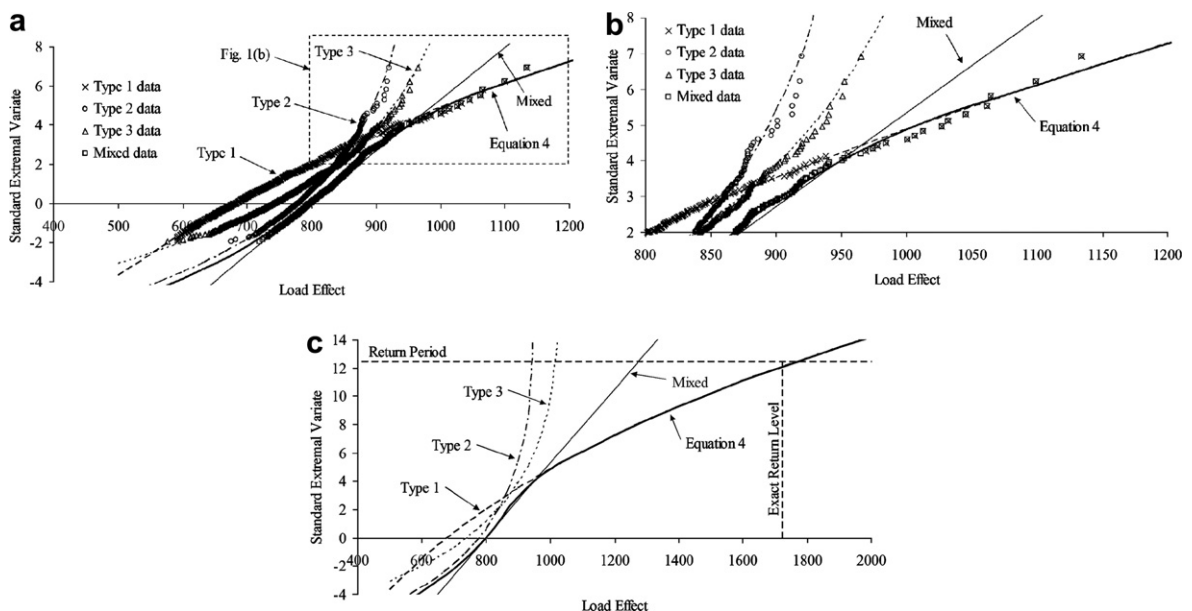


Fig. 1. Maximum-per-day simulated data from Example 1 on Gumbel probability paper: (a) detail of simulation period showing data; (b) detail of extreme values; and (c) extrapolation to return level (omitting the data points for clarity).

of ‘load effect’ becomes large – greater than about 950 as shown in Fig. 1b – the probabilities of exceedance of types 2 and 3 events get very small and the composite distribution converges towards the type 1 distribution. The characteristic value is found from Eq. (6) to be 1762, very close to the exact solution. The difference arises because the fitted distribution incorporates random sampling variation from the prescribed parent distributions.

The conventional approach is to mix data from a number of different event-types and identify the maximum-per-day, regardless of type. For each day of the simulated 1000 days, the maximum value is obtained and plotted in Fig. 1b, together with the maximum likelihood estimated GEV distribution. The low frequency of type 3 events means that this event type is not well sampled in the mixed distribution, a phenomenon that results in rare but important event types being poorly reflected in the results. The characteristic load effect is found to be 1272 from the conventional approach, 26% less than the exact solution. As the source data are mixed, the assumption of convergence to a single GEV distribution is not valid and the calculated characteristic value is not accurate.

In this example, users of the conventional approach have good evidence of the poor result from the quality of the fit in the tail. While the high type 1 event values are identified, they represent relatively few points overall. The vast majority of data points exhibit a linear trend in the mixture and these points dominate the mixed fit, resulting in a distribution that is not sympathetic to the correct trajectory of the greater load effect. It should be noted that this situation can be improved by weighting the GEV fit in the tail region, as proposed by Castillo [22].

The two other examples are presented in Appendix II. In Example 2, the conventional approach leads to a GEV distribution with flatter curvature which results in overestimation of the exact answer by 5.4%. In Example 3 the dominant event type is rare and poorly sampled leading to a very poor estimate of the characteristic value from the conventional approach.

### 3. Practical application

#### 3.1. Weigh-in-Motion data and load effect simulation

Realistic load effect data are used to assess the implications of Eq. (4) and to compare the results to those obtained using the conventional approach. For this purpose, Weigh-in-Motion (WIM) data were taken from the A6 motorway near Auxerre, France. Weight and dimension data were collected for 36,373 trucks travelling in the slow lanes of the 4-lane motorway. It is acknowledged that this is insufficient data for a reliable calculation of characteristic load effect. However, it is sufficient to provide realistic data for the comparisons which follow. The relative frequency of each type of truck (by number of axles) was used in the simulations. The recorded GVW data were modelled as a multi-modal (maximum of 3 modes) Normal distribution, as were the axle weights of 2- and 3-axle trucks. For 4- and 5-axle trucks, the percentage weight of the individual axles were modelled as Normal as was the tandem/tridem group for 12 different intervals of GVW. Individual axles of a group were assumed to have equal weight. Axle spacings were modelled as uni- or bi-modal Normal distributions, depending on the shape of the histogram. The small percentage (<1%) of 6- and more axle trucks were not modelled due to insufficient data. It is possible that these trucks may well be critical in the assessment of actual loads, though preliminary studies suggest that it is not sensitive [23].

Many authors [24–27] suggest that traffic may be approximated as a series of ‘homogenous’ days in which average hourly flow, averaged for a particular hour over many days, is used. The simulations carried out in this study assume this type of day. Speed is modelled as a Normal distribution and considered independent of truck type and to be uncorrelated with GVW. Finally, headways less than 1.5 s are assumed to be independent of flow as found by OBrien and Caprani [28]. On the other hand, headways in the 1.5–4 s range are fitted to the measured Cumulative Distribution Functions appropriate to the flow closest to the average hourly flow for each hour.

Three load effects are considered for bridge lengths in the range, 20–50 m:

- *Load effect 1*: bending moment at the mid-span of a simply supported bridge.
- *Load effect 2*: left support shear in a simply-supported bridge.
- *Load effect 3*: bending moment at central support of a two-span continuous bridge.

To minimise computing requirements only significant crossing events (SCEs) were processed. SCEs are defined as multiple-truck presence events and single truck events with GVW in excess of 40 tonnes. Single truck events with lesser GVWs were found to not feature in the maximum-per-day load effect data. When an SCE is identified, the truck(s) are moved in 0.02 s intervals across the bridge and the maximum load effects for the event identified.

### 3.2. Parent distribution of load effect data

The maximum load effect in a BLE,  $S_i$ , is the maximum load effect over the time period of the event. To determine the form of these parent distributions,  $S_i$ , for each event type, 30 years of truck traffic was simulated and fitted to a range of distributions. For 1- and 2-truck events, this resulted in a very large database of load effects, considerably more than is necessary to determine the cumulative distribution function. In these cases, the first approximately 65,500 load effect values were used to find the distributions. For 3- and 4-truck events, there was enough data to discern a clear trend for the bridge lengths considered in this study (20–50 m). However, fewer than twenty 5-truck events were registered in the 30 year period for bridge lengths of 40 m and none at all for lesser lengths. It was only for 50 m bridges that there was sufficient 5-truck event data to identify a trend.

To illustrate an imperfect result, the histogram for Load Effect 1 for 2-truck events on a 20 m span bridge is given in Fig. 2 together with maximum likelihood fits to several statistical distributions. GEV is the best of the maximum likelihood fits to the data for 39 out of 51 load effects and bridge lengths – the associated likelihood is greater than the corresponding likelihoods for all other distributions. GEV is close to the best in the remaining 12. It is therefore assumed that  $S_i$  is GEV or near-GEV distributed. Consequently, by the stability postulate [14,29,30],  $\hat{S}$ , the maximum of a number of  $S_i$ , is GEV distributed, for any number,  $f_i n_d$ .

### 3.3. Comparison of results with conventional approach

For the three load effects described and bridge lengths from 20 to 50 m, characteristic values calculated from Eq. (6) are compared with those found by the conventional approach. Theoretical examples [31] showed that reasonable estimates of known distributions are found from sample sizes of 1000 and above. Typical results from 1000 days of simulation are illustrated in Fig. 3. The daily maxima by event type (number of trucks involved) are plotted in Fig. 3a with the individual maximum-likelihood fits. Within the 1000 day simulation period, 2- and 3-truck events result in most of the daily maxima. However, different trends are evident in each of the data sets. It is of particular interest that the 4-truck event data, while contributing little to the daily maxima, shows a trend that indicates that it will feature strongly in a 1000 year return period. The quality of the fit to the 2- and 3-truck data is imperfect in the tail but this is the result of a small number of data points and is not representative of the general trend. In any case, the characteristic value is much more strongly influenced by 4-truck than 2- or 3-truck events.

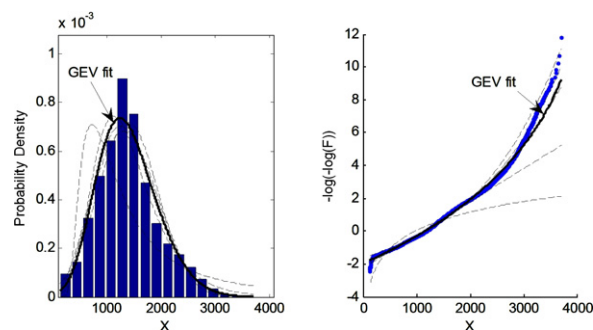


Fig. 2. Parent distribution of load effect 1 due to 2-truck events on a 20 m bridge (fits to alternative distributions shown dashed).

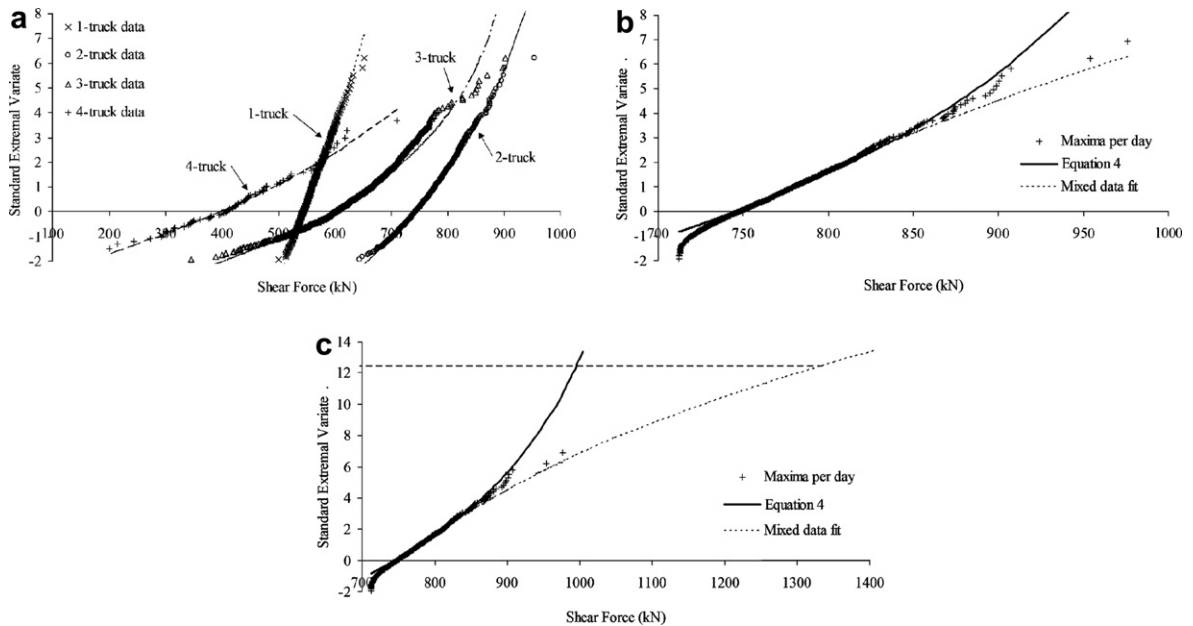


Fig. 3. Results for load effect 3 on 30 m long bridge: (a) daily maxima by event type; (b) mixed daily maxima; and (c) mixed daily maxima extrapolation to characteristic values.

The mixed maximum-per-day data are illustrated in Fig. 3b with the conventional approach and the fit by event type. The mixed data appears to fit better to a GEV distribution than the new approach. However, this is in fact an over-fitting to a mixture of data and is not representative of the four underlying trends shown in Fig. 3a. The conventional approach is in fact following a trend supported by the two most extreme data points which are the result of 2-truck events. There are pronounced differences in the

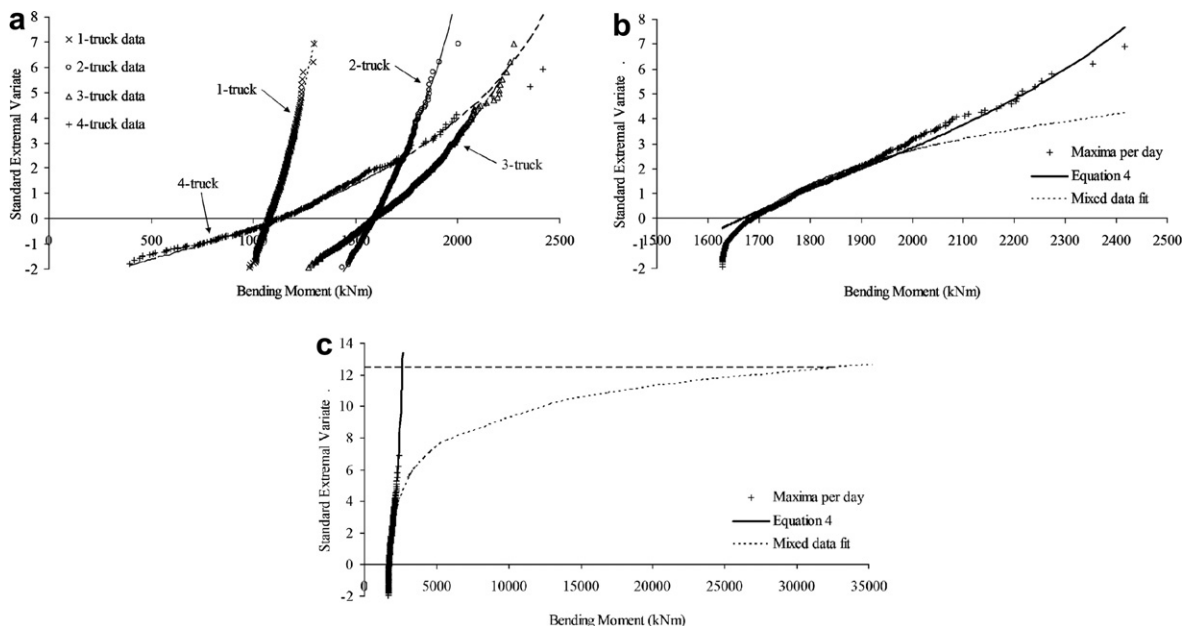


Fig. 4. Results for load effect 2 in a 40 m long bridge: (a) daily maxima by event type; (b) mixed daily maximal; and (c) mixed daily maxima extrapolation to characteristic values.

Table 2  
Comparison of 1000-year characteristic values

Load effect	Span	New approach	Conventional approach	Difference relative to new approach (%)
1	20	4103	4692	+14
	30	7093	10,250	+45
	40	11,033	28,532	+159
	50	13,968	62,132	+345
2	20	1069	1216	+14
	30	1537	3217	+109
	40	2614	32,525	+1144
	50	3564	18,567	+421
3	20	877	958	+9
	30	995	1333	+34
	40	1056	2415	+129
	50	1200	5811	+384

characteristic values when the 1000 days of data is used to predict the 1000 year extreme – see Fig. 3c. The conventional approach predicts a characteristic load effect of 1333, 34% in excess of 995, the corresponding value predicted by the new approach.

For Load Effect 2 in a 40 m bridge, different types of event feature as can be seen in Fig. 4. In this longer bridge, 3-truck events govern for much of the 1000 day simulation period and 4-truck events are more prominent than in the previous example.

The mixed maximum-per-day data are illustrated in Fig. 4b. In the left tail region – between 1600 and 1650 – the daily maxima come from a mixture of 2-, 3- and 4-truck events (see also Fig. 4a). This causes the strong downward curvature in the data. The fit to the mixed data is influenced strongly by this left-tail data with the result that it fits very poorly in the right tail. The implications are dramatic as can be seen when the trend is extended to the return level in Fig. 4c. Fortunately, in this case, unlike the previous one, the poor fit in the tail region will be evident to a user of the conventional approach and it can be addressed to some extent by biasing the fit in favour of the tail [22].

A summary of results is presented in Table 2. In all cases, the conventional approach is conservative relative to Eq. (4); in some cases very much so. Of course this may not always be the case.

It is clear from Figs. 3 and 4 that it is not reasonable to assume that 2-truck loading events govern the design of short to medium span bridges. Clearly 4-truck events play an important role. Further, when more than 1000 days of data are simulated, events involving more than four trucks emerge but are typically characterised by multiple short trucks with few axles and low GVW [31].

#### 4. Conclusions

Load effects in bridges result from single truck crossings or multiple-truck presence events which are mixtures of different statistical distributions. This paper reviews the procedure by which load effects from various multiple-truck presence events are statistically combined. An equation, used in the past for other applications, is derived in the context of bridge traffic loading. Theoretical examples, for which the exact solution is known, are used to demonstrate the inaccuracies that result from calculations of characteristic value based on mixtures of data sets.

Real traffic data are used to demonstrate the implications of the conventional approach of extrapolating from maximum-per-day load effects which arise from a mixture of truck crossing and meeting event types. The differences between the conventional and the new approach are great. Some inaccuracies are the result of an over-fitting to data outside the right tail region, a phenomenon which can be detected and addressed. However, other differences are due to underlying trends in rare event types which do not surface in 1000 days of simulations. An example shows that 4-truck meeting events which hardly feature in the maximum-per-day data are most important and have a great influence on the 1000 year characteristic value.



## Appendix I

### The relationship between Eqs. (3) and (4)

If only 1- and 2-truck events are considered, and (3) reduces to a binomial expansion:

$$P[\widehat{S} \leq s] = [f_1 \cdot F_1(s) + f_2 \cdot F_2(s)]^{n_d} = \sum_{k=0}^{n_d} \binom{n_d}{k} f_1^k f_2^{n_d-k} F_1^k(s) F_2^{n_d-k}(s) \quad (8)$$

It is well known that a binomial distribution of the form,

$$(f_1 + f_2)^{n_d} = \sum_{k=0}^{n_d} \binom{n_d}{k} f_1^k f_2^{n_d-k} \quad (9)$$

converges to the Normal distribution (for  $n_d f_1 \geq 10$  approximately) with mean  $n_d f_1$  and variance  $n_d f_1 f_2$  [12]. The use of the Normal distribution approximation removes the requirement that  $n_d f_j$  be an integer. Hence, the expansion is symmetrical with equal terms on either side of the mean. Thus, it can be expressed with terms in order of decreasing magnitude, as

$$(f_1 + f_2)^{n_d} = \binom{n_d}{n_d f_1} f_1^{n_d f_1} f_2^{n_d f_2} 3 + 2 \sum_{k=1}^{n_d f_2} \binom{n_d}{n_d f_1 + k} f_1^{n_d f_1 + k} f_2^{n_d f_2 - k} \quad (10)$$

Eq. (8) can be expressed in a similar form but, in this case, only the combined coefficient and  $f_1^{n_d f_1 + k} f_2^{n_d f_2 - k}$  terms are symmetrical:

$$(f_1 F_1 + f_2 F_2)^{n_d} = \binom{n_d}{n_d f_1} f_1^{n_d f_1} f_2^{n_d f_2} F_1^{n_d f_1} F_2^{n_d f_2} + \sum_{k=1}^{n_d f_2} \binom{n_d}{n_d f_1 + k} f_1^{n_d f_1 + k} f_2^{n_d f_2 - k} [F_1^{n_d f_1 - k} F_2^{n_d f_2 + k} + F_1^{n_d f_1 + k} F_2^{n_d f_2 - k}]$$

where the distributions  $F_i(s)$  are written as  $F_i$  for clarity. As  $F_1(s)$  and  $F_2(s)$  are very close to unity for extrapolations to long return periods, they can be expressed as

$$F_i(s) = 1 - \delta_i \quad \text{where } i = 1, 2 \quad (12)$$

for small  $\delta_i$ . A Taylor series expansion gives

$$F_i^m = (1 - \delta_i)^m = 1 - m\delta_i + \frac{1}{2}m(m-1)\delta_i^2 - \dots \quad (13)$$

which is well approximated by the first two terms. Introducing the functions,

$$g_i^{+k} \equiv 1 - (n_d f_i + k)\delta_i \quad \text{and} \quad g_i^{-k} \equiv 1 - (n_d f_i - k)\delta_i$$

Eq. (11) then becomes

$$(f_1 F_1 + f_2 F_2)^{n_d} = \binom{n_d}{n_d f_1} f_1^{n_d f_1} f_2^{n_d f_2} (1 - n_d f_1 \delta_1)(1 - n_d f_2 \delta_2) + \sum_{k=1}^{n_d f_2} \binom{n_d}{n_d f_1 + k} f_1^{n_d f_1 + k} f_2^{n_d f_2 - k} (g_1^{-k} \cdot g_2^{+k} + g_1^{+k} \cdot g_2^{-k}) \quad (14)$$

Ignoring second-order terms,  $(g_1^{-k} \cdot g_2^{+k} + g_1^{+k} \cdot g_2^{-k})$  reduces to  $(1 - n_d f_1 \delta_1)(1 - n_d f_2 \delta_2)$ . Using Eq. (10), (14) then becomes

$$(f_1 F_1 + f_2 F_2)^{n_d} = (f_1 + f_2)^{n_d} (1 - n_d f_1 \delta_1)(1 - n_d f_2 \delta_2) \quad (15)$$

Given that  $f_1 + f_2 = 1$ , and again using Eq. (13), this can be simplified to:

$$P[\widehat{S} \leq s] = F_1^{n_d f_1}(s) \cdot F_2^{n_d f_2}(s) \quad (16)$$

If the parent distributions,  $F_1(s)$  and  $F_2(s)$ , are extreme value distributed, then by the stability postulate [13,28,29],  $F_1^{n_d f_1}(s)$  and  $F_2^{n_d f_2}(s)$  are also extreme value, regardless of how small is the power to which they are raised. If  $F_1(s)$  and  $F_2(s)$  are not GEV distributed, then  $F_1^{n_d f_1}(s)$  and  $F_2^{n_d f_2}(s)$  may still converge to an

extreme value distribution if  $n_d f_1$  and  $n_d f_2$  are sufficiently large with respect to the particular parent distributions. If such conditions are satisfied, Eq. (16) becomes

$$P[\widehat{S} \leq s] = G_1(s)G_2(s) \tag{17}$$

where  $G_1(s)$  and  $G_2(s)$  are extreme value distributions.

For  $n_t$  event types, a corresponding result can be found using the multivariate Normal distribution approximation to the multinomial distribution [32]:

$$P[\widehat{S} \leq s] = \prod_{j=1}^{n_t} G_j(s) \tag{18}$$

which is the same as Eq. (4), found by other authors through different approaches [11,14–16].

**Appendix II**  
**Further theoretical examples**

Example 2, illustrated in Fig. 5 (see also Table 1), represents a mixture of types 1 and 2 events. Similarly to Example 1, 1000 samples points representing daily maximum load effect values from each event-type are obtained. Also, the extrapolation period is as for Example 1. In this case, the data are roughly centred about the point where the types 1 and 2 event curves intersect. As a result, the conventional approach using the mixed data identifies an even spread of maxima from both event types in the simulation period. In the right tail region it follows a similar trend to the type 2 data. In this example, type 2 events are dominant in both the simulation period and the extrapolation period. The mixing of the data near the point of intersection means that the conventional approach has a flatter curvature than the actual governing distribution and consequently it overestimates (2389) the exact answer determined from Eq. (3) to be 2266. The new approach is sympathetic to the curvature of the governing distribution and gives a characteristic value quite close (2253) to the exact answer. Again, sampling variation can account for the difference observed.

Example 3, illustrated in Fig. 6 (see also Table 1), demonstrates a case where the dominant distribution – type 1 – is unbounded (negative shape factor,  $\xi$ ) but the GEV fit to the mixture is bounded. The result is a

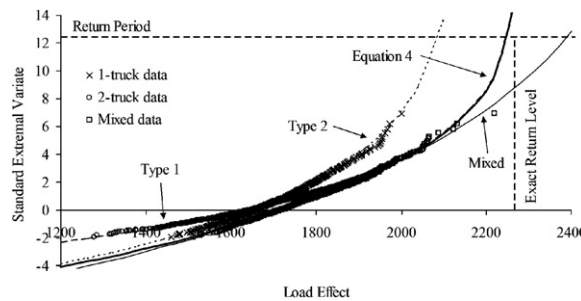


Fig. 5. Maximum-per-day simulated data from Example 2 on Gumbel probability paper.

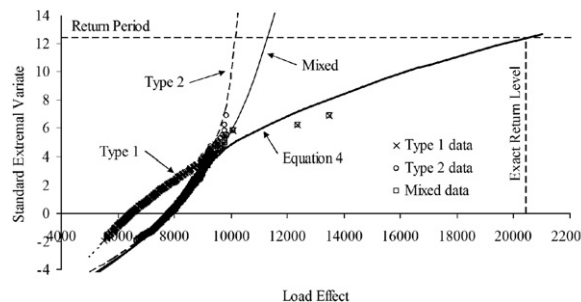


Fig. 6. Maximum-per-day simulated data from Example 3 on Gumbel probability paper.

dramatic difference in the results. The curve of the governing type 1 distribution does not cross the type 2 curve until near the end of the simulation period. As a result, there are only two points that do not fit well to the conventional fit to the mixture of data. The conventional approach gives a characteristic value of 11,303 as opposed to the exact answer, determined from Eq. (3) to be 20,450, and the new approach, which is 20,500. It is also noteworthy that the inaccuracy of the result is not readily apparent from the data in the simulation period.

## References

- [1] BD 21, Design manual for roads and bridges, vol. 3, Section 4, Part 3, Department of Transport, United Kingdom; 1993.
- [2] Cooper DI. Development of short span bridge-specific assessment live loading. In: Das PC, editor. Safety of bridges. Thomas Telford; 1997. p. 64–89.
- [3] Rubenstein RY. Simulation and the Monte Carlo method. John Wiley and Sons; 1981.
- [4] Bruls A, Croce P, Sanpaolesi L, Sedlacek G. ENV1991 – Part 3: traffic loads on bridges; calibration of load models for road bridges. In: Proceedings of IABSE colloquium, Delft, The Netherlands, IABSE-AIPC-IVBH; 1996. p. 439–53.
- [5] Nowak AS. Live load model for highway bridges. *Struct Saf* 1993;13:53–66.
- [6] Nowak AS, Hong YK. Bridge live load models. *J Struct Eng, ASCE* 1991;117(9):2757–67.
- [7] Bailey SF, Bez R. Site specific probability distribution of extreme traffic action effects. *Probabilist Eng Mech* 1999;14(1):19–26.
- [8] O'Brien EJ, Sloan TD, Butler KM, Kirkpatrick J. Traffic load fingerprinting of bridges for assessment purposes. *Struct Eng* 1995;73(19):320–4.
- [9] Moyo P, Brownjohn JM, Omenzetter P. Highway bridge live loading assessment and load carrying estimation using a health monitoring system. In: Balageas DL, editor. Proceedings of the first European workshop on structural health monitoring. Cachan (Paris), France; 2002.
- [10] Ghosn M, Moses F. Markov renewal model for maximum bridge loading. *J Eng Mech, ASCE* 1985;111(9):1093–104.
- [11] Crespo-Minguillón C, Casas JR. A comprehensive traffic load model for bridge safety checking. *Struct Saf* 1997;19:339–59.
- [12] Gumbel EJ. Statistics of extremes. Columbia University Press; 1958.
- [13] Feller W. An introduction to probability theory and its applications, 2nd ed., vol. I. New York: Wiley; 1957.
- [14] Galambos J. The asymptotic theory of extreme order statistics. New York: John Wiley and Sons; 1978.
- [15] Gomes L, Vickery BJ. Extreme wind speeds in mixed climates. *J Wind Eng Ind Aerodyn* 1977/1978;2:331–44.
- [16] Harman DJ, Davenport AG. A statistical approach to traffic loading on highway bridges. *Can J Civil Eng* 1979;6:494–513.
- [17] Cook NJ, Harris RI, Whiting R. Extreme wind speeds in mixed climates revisited. *J Wind Eng Ind Aerodyn* 2003;91:403–22.
- [18] Coles SG. An introduction to statistical modeling of extreme values. London: Springer-Verlag; 2001.
- [19] Lehman EL. Testing statistical hypotheses. 2nd ed. New York: Wiley Series in Probability and Mathematical Statistics; 1986.
- [20] Young QH. Likelihood ratio tests for model selection and non-nested hypotheses. *Econometrica* 1987;57(2):307–33.
- [21] EC 1. Basis of design and actions on structures, Part 3: traffic loads on bridges, European Prestandard ENV 1991-3: European Committee for Standardisation, TC 250, Brussels; 1994.
- [22] Castillo E. Extreme value theory in engineering. Academic Press; 1988.
- [23] Getachew A, O'Brien EJ. Sensitivity of predicted bridge traffic load effects to the tails of truck weight distributions. In: Parke GAR, Disney P, editors. Proceedings of the fifth international conference on bridge management. London: University of Surrey, Thomas Telford; 2005. p. 275–82.
- [24] Fu G, Hag-Elsafi O. Bridge evaluation for overloads including frequency of appearance. In: Favre L, Mébarki A, editors. Applications of statistics and probability. Rotterdam; 1995. p. 687–92.
- [25] Hallenbeck M. Seasonal patterns of truck loads and volumes in the United States. In: Proceedings of the first European conference on weigh-in-motion of road vehicles. ETH Zürich, Switzerland; 1995. p. 121–9.
- [26] Cooper DI. The determination of highway bridge design loading in the United Kingdom from traffic measurements. In: Jacob B et al., editors. Pre-proceedings of the first European conference on weigh-in-motion of road vehicles. E.T.H., Zürich; 1995. p. 413–21.
- [27] Grave SAJ. Modelling of site-specific traffic loading on short to medium span bridges, PhD Thesis. Dept. of Civil Engineering, Trinity College Dublin; 2001.
- [28] O'Brien EJ, Caprani CC. Headway modeling for traffic load assessment of short-to-medium span bridges. *Struct Eng* 2005;83(16):33–6.
- [29] Gnedenko B. Sur la distribution limitée u terme maximum d'une série aléatoire. *Ann Math* 1943;44:423–53.
- [30] Fisher RA, Tippett LHC. Limiting forms of the frequency distribution of the largest or smallest number of a sample. *Proc Cambridge Philos Soc* 1928;XXIV(Part II):180–90.
- [31] Caprani CC. Probabilistic analysis of highway bridge traffic loading, Ph.D. Thesis. School of Architecture, Landscape and Civil Engineering. Ireland: University College Dublin; 2005.
- [32] Bishop YMM, Fienberg SE, Holland PW. Discrete multivariate analysis: theory and practice. Cambridge, Massachusetts: MIT Press; 1975.